

## Supplementary Information

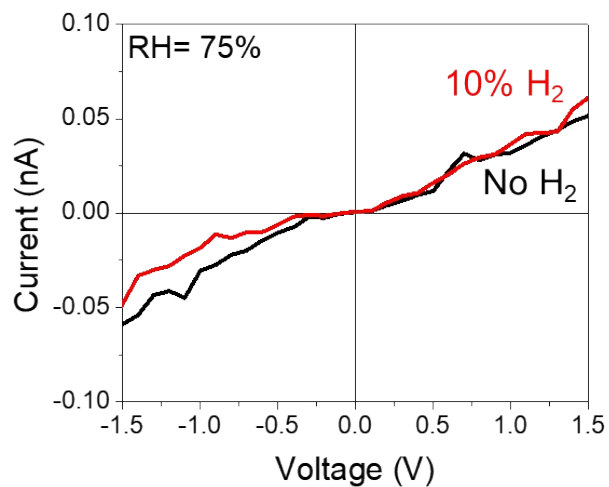
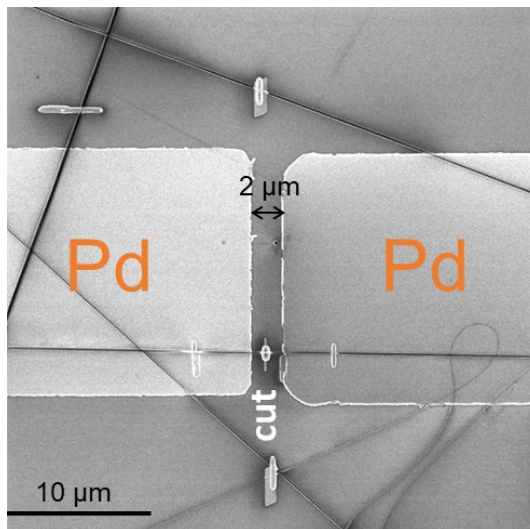
Enhanced protonic conductivity and IFET behavior in individual proton-doped  
electrospun chitosan fibers

Woo-Kyung Lee,<sup>\*a</sup> Jeremy J. Pietron,<sup>a</sup> David A. Kidwell,<sup>a</sup> Jeremy T. Robinson,<sup>b</sup> Christopher L.  
McGann,<sup>c</sup> Paul E. Sheehan<sup>a</sup> and Shawn P. Mulvaney<sup>a</sup>

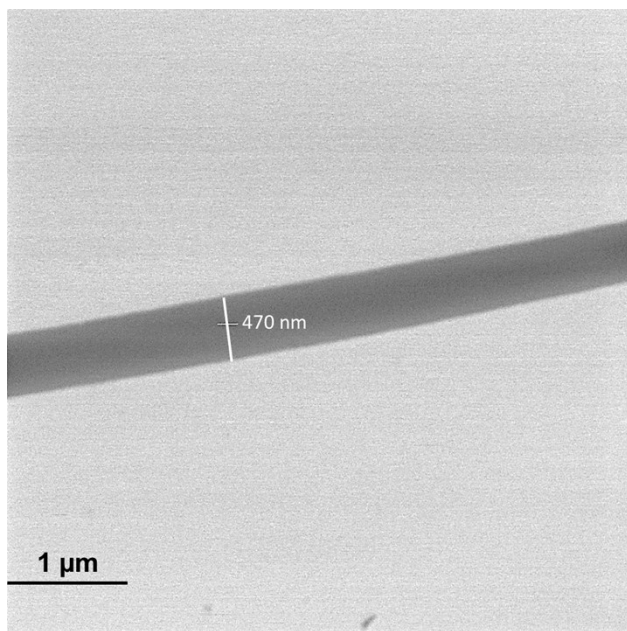
<sup>a</sup>*Chemistry Division, U.S. Naval Research Laboratory, Washington, DC, 20375 USA*

<sup>b</sup>*Electronics Science and Technology Division, U.S. Naval Research Laboratory, Washington,  
DC, 20375 USA*

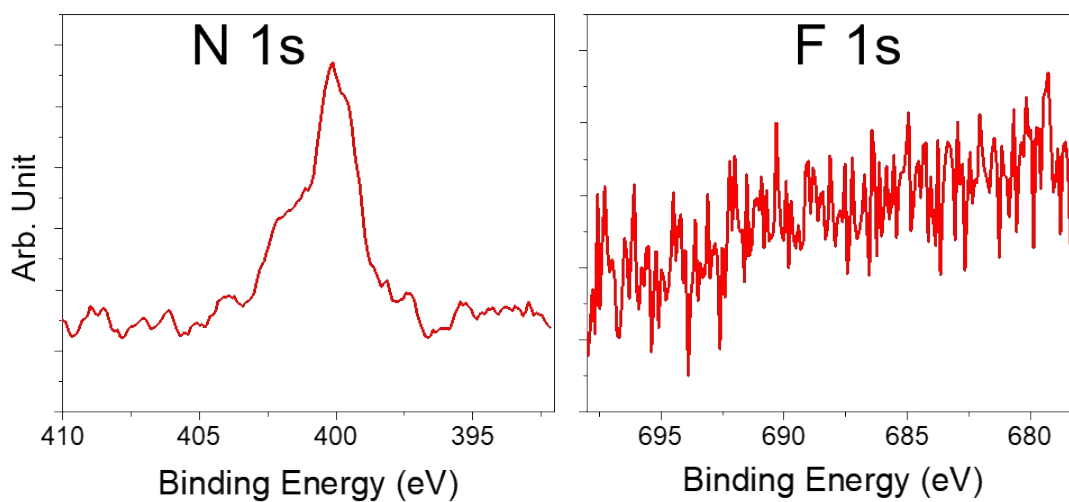
<sup>c</sup>*American Society for Engineering Education Postdoctoral Fellow, Chemistry Division, U.S.  
Naval Research Laboratory, Washington, DC 20375, United States*



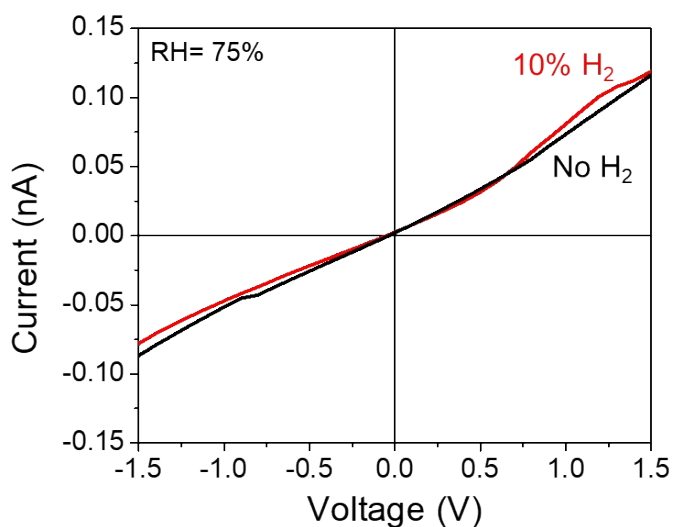
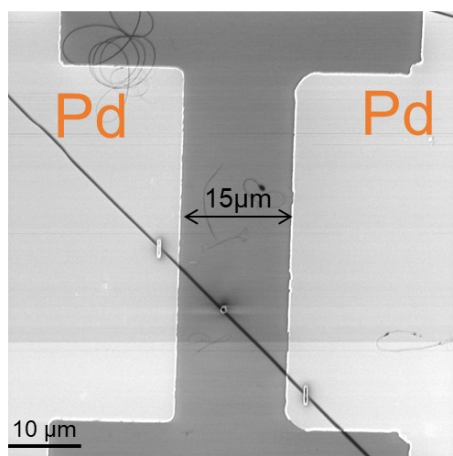
SI 1. Cutting electrospun chitosan fibers with helium ion microscope (HIM). No protonic conduction behavior was observed under 10% hydrogen atmosphere after cutting fibers between Pd protodes, *i.e.* no resistance change due to the presence or absence of hydrogen. ( $R \approx 24 \text{ G}\Omega$ )



SI 2. HIM image of electrospun chitosan fiber.



SI 3. XPS analysis of the medium density, electrospun chitosan fibers after TFA residue removal by NaOH, acetone, and subsequent drying under vacuum. The protonated amine signature and fluorine 1S peaks were reduced by the treatment.



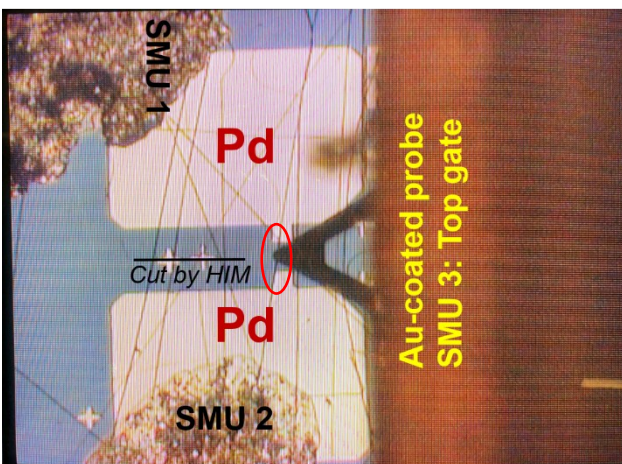
SI 4. The I-V measurement after TFA residue removal by NaOH/H<sub>2</sub>O, acetone, and subsequent drying under vacuum. There is no proton conductivity with the presence of 10% hydrogen atmosphere.

**SI 5. Details of the digital simulation of I–V behavior of chitosan fiber-based devices under humid (70% RH) flowing 10% H<sub>2</sub> / 90% N<sub>2</sub>:** Two approaches to digital simulation of the hydrogen oxidation reaction (HOR) chemistry at the chitosan nanofiber-based protonics devices were tried in the present study. In our previous study,<sup>1</sup> we used a semi-infinite linear diffusion approximation for H<sub>2</sub> and H<sup>+</sup> diffusion in the chitsan films, which worked well with the devices that featured films over 100 μm in width and inter-protode gaps of 2–64-μm gaps. The relatively large cross-sectional area of the films (~7 x 10<sup>-5</sup> cm<sup>2</sup>) compared to the chitosan fibers allowed them to be treated approximately as a semi-infinite reservoir of the electrochemical reagents H<sub>2</sub> and H<sup>+</sup> for simulation purposes. In some detail, the semi-infinite linear diffusion approach assumes that a diffusion gradient forms that is defined by two boundary conditions: (1) at the electrode surface, the releative concentrations of the oxidized and reduced species are determined by electrode potential and the Nernst equation, which is  $E = E^0 + (RT/nF)\ln[a_{OX}/a_{RED}]$ , where E is the applied electrode potential, E<sup>0</sup> is the formal potential for the electrochemical reaction, R is the gas constant, T is temperature, F is Faraday's constant, and a<sub>OX</sub> and a<sub>RED</sub> are the activities for the oxidized an reduced species in the electrochemical reaction; (2) at the outer boundary of the diffusion layer, the concentration of active species is defined by the bulk medium concentration; and (3) the time-varying current is determined by solving Fick's second law, which is  $\delta C(x,t)/\delta t = D\delta^2 C(x,t)/\delta x^2$ , where C is the concentration of the electroactive species, x is the linear thickness of the diffusion layer (which expands during the course of experimental time.) At any given point in time, the current is simply described by Fick's first law of flux, which is  $J \text{ (mol/s cm}^2\text{)} = D(\delta C/\delta x)$  and  $I \text{ (current)} = nFAJ$ , where n is the number of electrons transferred in the electrochemical reaction, A is electrode area and F is again Faraday's constant.  $\delta C/\delta x$  is the concentration gradient between the electrode surface and the bulk medium. The second law solution is needed to solve for the fact that the thickness of the diffusion layer evolves in time in potential step and potential sweep experiments. More detailed derivations of these conditions can be found in *Electrochemical Methods: Fundamentals and Applications*, by A.J. Bard and L. Faulkner, John Wiley and Sons, New York, 1980, Chapters 5 and 6. The framing of the digital simulation of the time-dependent currents can be found in the same reference in Appendix B, starting on p. 675.

For the chitosan fiber-based devices, the cross sectional area between the fiber and the protodes were typically on the order of  $5 \times 10^{-10} \text{ cm}^2$ —five orders of magnitude smaller than that for the films in the previous study. The data for the fibers could not be fit well using semi-infinite linear diffusion models, and was much better fit modeling the electrochemistry as confined to the contact area between the chitosan fibers and the Pd protodes, as a fixed film volume. This suggests that the rate-determining process in the chitosan fiber-based protonics devices was the electrochemical HOR at the individual  $\sim 5 \times 10^{-10} \text{ cm}^2$  Pd/chitosan interfaces, and not micrometer-scale diffusion of the  $\text{H}_2$  from the volume in chitosan fiber spanning the inter-protode gap to the protodes, thus we chose a more geometrically constrained model for the digital simulations in the present study, which still solves Fick's second law, but within the spatial constraints appropriate to the dimensions of the electrospun fibers. Using a finite boundary diffusion model in the Digisim<sup>®</sup> 3 digital simulation software (BASi), we chose the thickness of the individual fibers as the diffusion layer thickness and the apparent contact area between the chitosan fibers and the Pd protodes. Best fits of the simulated data to the experimental I–V curves were achieved using a concentration of  $\text{H}^+$  of 0.1 M, which is  $\sim 100$ -fold higher than that modeled previously for chitosan films cast from acetic acid.<sup>1</sup> This is well-within expectation, because as described in the results and discussion of this manuscript, the chitosan fibers are spun from trifluoroacetic acid solutions, and the acidity of TFA ( $\text{pK}_a = 0.22$ ) is substantially higher than that of acetic acid ( $\text{pK}_a = 4.7$ ). This  $\text{pK}_a$  difference result in an approximately 500-fold higher  $\text{H}^+$  concentration in TFA-derived PCMs under ideal (dilute-solution) conditions. Our doped, polymeric proton-conducting materials (PCMs) do not comprise dilute solutions, but both the acetic acid-derived chitosan PCMs and TFA-derived chitosan PCMs are substantially hydrated under the 75% RH atmospheres in the present study, and thus should qualitatively obey the predictions of relative  $\text{H}^+$  concentration derived from the respective  $\text{pK}_a$  values. Thus we deemed a best-fit of  $\text{H}^+$  concentration of 0.1 M—100-fold higher than for acetic-acid derived chitosan PCMs—to be reasonable. The more surprising best fit was for the  $\text{H}_2$  concentration, which was  $\sim 7 \text{ M}$ . This high concentration implies that the  $\text{H}_2$  concentration gradient is on the Pd side of the Pd/chitosan interface. Hydrogen-saturated Pd can reach mole fractions from a few percent of up to  $\sim 50\% \text{ H}_2$ .<sup>2</sup> The concentration of Pd atoms in solid Pd is 112 M, thus at a few percent of saturation, 7 M  $\text{H}_2$  concentration in Pd is very reasonable. The treatment is necessarily inexact:  $\text{H}_2$  will certainly be diffusing to the Pd/chitosan interface from both sides of the Pd/chitosan interface, whereas  $\text{H}^+$  will likely only approach from the

chitosan side, thus it is unclear whether the thickness of Pd protodes or the chitosan fiber is more appropriate for the finite diffusion layer. But taken together, the electrode HOR kinetics will be a product of the concentration of reactants, interfacial geometry, and layer thickness, and different combinations of these can give an identical mathematical product that accurately simulates the overall rate of the HOR reaction. Given that our fits produce an electrochemical HOR rate constant ( $k^0 = 2 \times 10^{-5} \text{ s}^{-1}$ ) that agrees so well with that modeled previously for chitosan films on protonics devices of completely different geometries,<sup>1</sup> modeled with completely different diffusion assumptions, we conclude that our assumptions and approximations are reasonable.

- (1) Robinson, J. T.; Pietron, J. J.; Blue, B.; Perkins, F. K.; Josberger, E.; Deng, Y.; Rolandi, M. Electrical and electrochemical characterization of proton transfer at the interface between chitosan and PdHx. *Journal of Materials Chemistry C* **2017**, *5*, 11083-11091.
- (2) Uluc, A. V.; Mol, J. M. C.; Terryn, H.; Bottger, A. J. Hydrogen sorption and desorption related properties of Pd-alloys determined by cyclic voltammetry. *Journal of Electroanalytical Chemistry* **2014**, *734*, 53-60.



SI 6. The experimental setup for a single chitosan fiber ionic field effect transistor (IFET) with atomic force microscope (AFM). The Au-coated, tip-less AFM probe was engaged directly onto the chitosan fiber (red circle), while other fibers across Pd electrodes were cut by HIM. The FET measurements were conducted by Keithely 4200 semiconductor analyzer.